Eur Radiol (2012) 22:1–8
DOI 10.1007/s00330-011-2169-4

BREAST

High-resolution spiral CT of the breast at very low dose: concept and feasibility considerations

Willi A. Kalender · Marcel Beister · John M. Boone · Daniel Kolditz · Sabrina V. Vollmar · Michaela C. C. Weigel

Received: 30 March 2011 / Revised: 9 May 2011 / Accepted: 23 May 2011 / Published online: 9 June 2011

Abstract
Objective Mammography, today's standard imaging approach, has deficits with respect to the superimposition of anatomical structures. Dedicated CT of the breast so far indicated that it can provide superior soft-tissue imaging, but that it still has significant limitations with respect to spatial resolution and dose. We have assessed novel dedicated breast CT technology.
Methods Based on simulations and measurements we developed novel technology which uses direct-conversion CdTe material and photon-counting electronics with 100 μm detector element size for close to 100% dose efficiency. We assessed the potential for the imaging of microcalcifications of 100 to 200 μm diameter and soft-tissue lesions of 1 to 5 mm diameter by simulations at dose levels between 1 and 6 mGy.
Results Microcalcifications of 150 μm and soft-tissue lesions of 2 mm diameter were found to be clearly detectable at an average glandular dose of 3 mGy. Separate displays are required for high-resolution microcalcification and for low-resolution soft-tissue analysis. Total CT data acquisition time will be below 10 s.
Conclusion Dedicated breast CT may eventually provide comprehensive diagnostic assessment of microcalcifications and soft-tissue structures at dose levels equivalent to or below those of two-view screening mammography.

Keywords Computed tomography (CT) · Breast · Image quality · Spatial resolution · Dose efficiency

Key points
– Breast CT allows diagnosing both microcalcifications and soft tissue in one acquisition.
– Microcalcifications of 100 to 150 μm are resolved.
– Soft tissue lesions down to 2 mm diameter are discernable.
– Dose levels of 2–4 mGy AGD conform with constraints imposed on screening.

W. A. Kalender (✉) · M. Beister · D. Kolditz · S. V. Vollmar · M. C. C. Weigel
Institute of Medical Physics, University Erlangen-Nürnberg,
Henkestr. 91,
91052 Erlangen, Germany
e-mail: willi.kalender@imp.uni-erlangen.de
URL: www.imp.uni-erlangen.de

J. M. Boone
Department of Radiology,
University of California Davis Medical Center,
Sacramento, CA, USA

Introduction

The early and reliable detection of breast carcinoma remains a challenge. Digital x-ray mammography is established as the primary investigation in breast cancer screening and diagnosis; however, there is intense debate regarding its performance [1–3]. Its sensitivity for lesion detection in the range of 62% to 88% [4] may be considered as questionable; in specific patient groups sensitivity is even lower and, for example, quoted as 58% for women under 49 years [5] and as low as 33% for women with genetically higher breast cancer risk [6]. Consequently, there is great interest in alternative approaches.

Digital tomosynthesis and magnetic resonance imaging (MRI) are of particular interest in this respect. Tomosynthesis of the female breast provides limited information in depth and initial clinical trials do not yet show convincing advantages over mammography [7–9]. MRI is of particular interest as it offers full 3D and dynamic imaging capabilities following the intravenous administration of contrast agents [1, 6]. However, it cannot reliably detect calcification and is complicated to perform when biopsies are involved.

The "perfect" breast imaging approach should meet with the demands summarized in Table 1, and CT is here considered as a candidate. Full 3D capabilities which are considered a necessity are ensured by its principle. Breast CT also provides adequate soft-tissue differentiation [10–12] and can offer accurate local tissue density values which are often considered important [13]. Contrast-enhanced imaging has also been demonstrated successfully [14]; dynamic imaging is not a problem either.

The big challenges are to meet demands no. 5 and 6, i.e. high resolution and good lesion detection in a single low-dose CT data acquisition . The demand for resolution of about 100 μm relates to the desired imaging of microcalcifications with a quality similar to or better than mammography. First prototypes of dedicated breast CT systems revealed inferior performance with respect to microcalcification due to their limited spatial resolution of about 300 μm [11, 12]. We demonstrated by micro-CT imaging of specimens that CT with high isotropic spatial resolution can provide the resolution for excellent assessment of microcalcification with a signal of above 5,000 HU at 60 kV [15].

The demand for an average glandular dose (AGD) of below 5 mGy as an upper limit relates to the demands imposed on two view mammographic screening in Europe [16]; it would also meet the limit of 6 mGy valid for the USA [17]. It is understood that, in general, dose may have to be increased if there is a valid indication such as diagnostic workup for cases of suspected breast cancer or for interventional procedures. Nevertheless, it appears desirable to stay within the limits imposed for screening where we can safely assume a very high benefit-to-risk ratio [18].

Demands no. 7 to 9 are predominantly engineering issues and are solvable. Breast CT avoids compression, which means an improvement of patient comfort. A biopsy option similar to what today's dedicated biopsy tables offer can be provided easily and, again, without compression; based on the 3D CT information it will provide the highest in targeting accuracy. The cost of such a CT system is estimated to be in the same order of magnitude as a tomosynthesis apparatus.

Table 1 Demands on imaging of the breast (adapted from [23])

1. Full 3D capability
2. Good soft-tissue differentiation
3. Accurate tissue density assessment
4. Dynamic contrast-enhanced imaging
5. High isotropic spatial resolution of 100 μm
6. Low patient dose with an AGD below 5 mGy
7. Patient comfort without breast compression
8. Integrated biopsy option
9. Low cost

Work on the concept of a novel dedicated breast CT system which could meet the demands stated in Table 1 started at the Institute of Medical Physics (IMP) in Erlangen around 2006 and was supported by grants from the European Union [19] and by the German National Science Foundation [20]; recently, research and development were started in cooperation with Artemis Imaging GmbH, a spinoff of the IMP, which was funded by the German Ministry of Education and Research [21].

In this special report, we describe the general physical and technical considerations on how to reach 100 μm spatial resolution with excellent low-contrast resolution using less than 5 mGy average glandular dose (AGD). The validation results in this study were obtained by simulations. We focus on the two most important tasks: soft-tissue lesion (STL) and microcalcification (μCa) detection.

Materials and methods

Novel dedicated breast CT concept

The basic design was derived by general considerations and simulations [15]. Initially we aimed at the use of standard flat detectors (Fig. 1a), but then decided on a spiral CT approach and a new detector design (Fig. 1b,c). The parameters of importance for image quality and dose simulations reported here are summarized in Table 2. The short distances from focal spot to center of rotation and to the detector are important both with respect to x-ray power demands and the size of the CT system. The field of measurement is 20 cm in diameter to accommodate the typical breast sizes of 8 to 18 cm [22]. The detector which is presently under development aims at 100% geometric and absorption efficiency. It uses directly converting cadmium telluride (CdTe) crystals in photon-counting mode with a detector pixel size of $(100\ \mu m)^2$. Absorption efficiency will be above 99% at the 60 kV setting planned, geometric efficiency will be close to 100% just the same since there is no division into single detector elements necessary for the direct converter [23]. In consequence, we can expect higher dose efficiency than for any clinical CT system. No signal time lag is to be expected due to the very high temporal resolution offered by CdTe. The detector uses a selectable low-energy threshold to eliminate electronic noise, dark current and low-energy scatter, which exceeds the performance of the scintillator detectors in use today. The detector height will be limited to about 5 to 8 cm to avoid large cone angles and high scatter intensities.

CT data acquisition modes

To achieve high dose efficiency, spiral CT data acquisition without oversampling effects is employed with 2,000 projec-

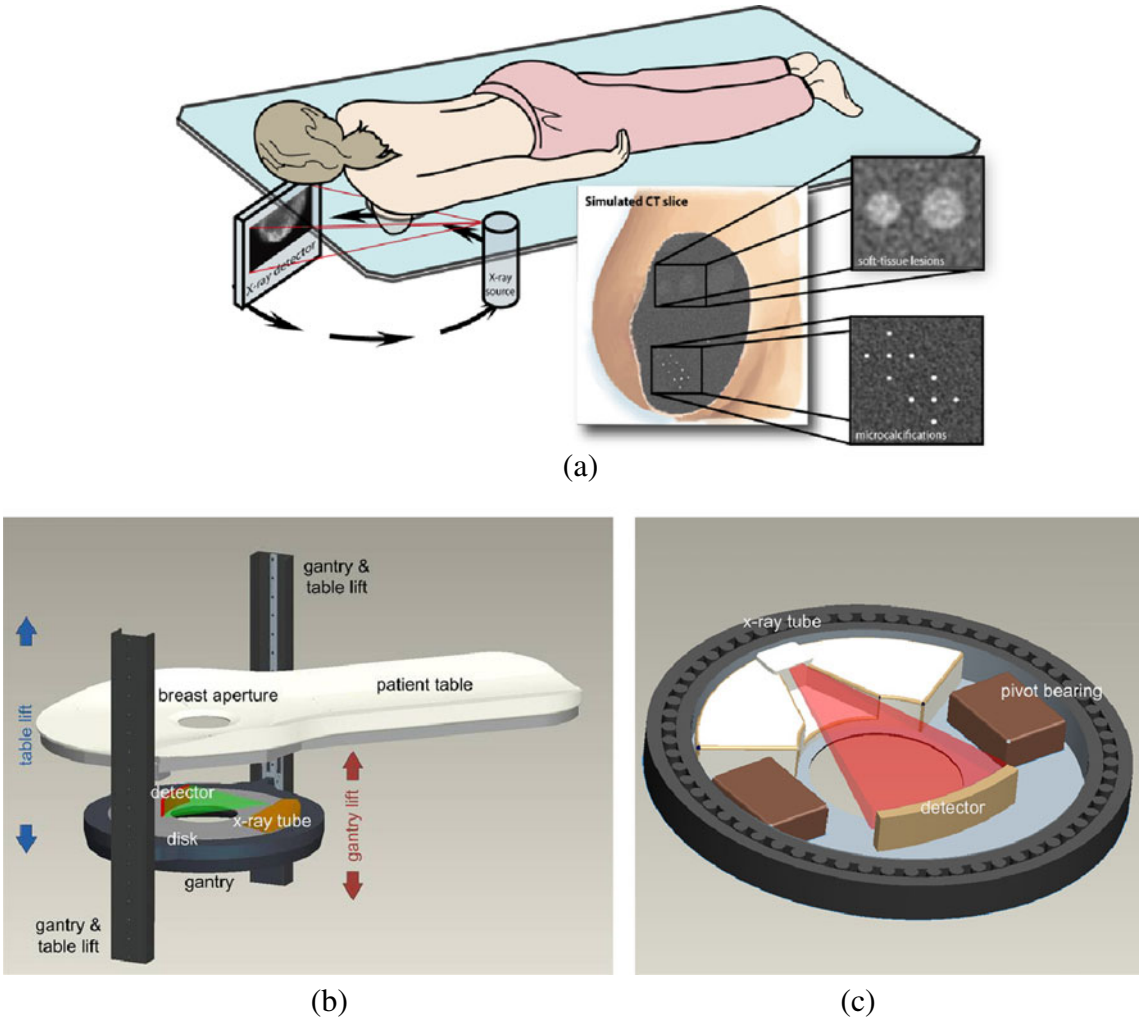

Fig. 1 Design concepts for the proposed breast CT with the patient positioned prone and only one breast exposed and examined at a time. (**a**) First concept with a standard flat detector [15]. Present design with the patient bed (**b**) and the gantry (**c**) moving up and down independently allowing for spiral acquisition and for easy patient access [23]

tions acquired per 360° with 2 s rotation time. We plan on using focal spot sizes of 100 μm and 300 μm at 60 kV with 3 mm aluminum filtration which was determined to be a dose-efficient and realizable solution for dedicated breast CT [24].

Table 2 Parameters of the novel CT system setup

Parameter	Value
Focus-Isocenter distance	300 mm
Detector-Isocenter distance	150 mm
Detector pixel size	$(100\ \mu m)^2$
Number of projections per 360°	2,000
Focal spot size	100 or 300 μm
Tube voltage	60 kV
Filtration	3 mm Al

Acquisition times per breast will be limited to 10 s or below; we plan for breast fixation to exclude motion effects.

If not stated differently, all the results presented below were obtained for 10 cm anatomical length with 60 kV and the mAs value adjusted to deliver an AGD of 3 mGy. Additionally, a volume-of-interest (VOI) mode [25] was investigated which aims at providing an initial overview CT data acquisition (OV) for the whole field of view with wide fan at lowered dose. In this mode, the reconstructed image has adequate image quality for a general orientation. A sub-volume of arbitrary position and size is then selected for closer investigation, e.g. a suspicious area with microcalcifications to be imaged at higher resolution or a lesion to be treated. The collimation is narrowed both in fan and in z-direction according to the selection of the sub-volume and one or several VOI CT data acquisitions are performed.

Image reconstruction

For image reconstruction we employed a standard Feldkamp-based filtered back-projection (FBP) software package (ImpactRecon, Artemis Imaging GmbH, Erlangen, Germany) with an experimental extension that provides a model-based iterative reconstruction (MBIR) method. In order to provide fast results for large datasets, both algorithms were implemented on modern graphics processing units (GPUs) using the "Compute Unified Device Architecture" (CUDA) framework from NVIDIA. The iterative method is based on the ordered subset convex (OSC) algorithm [26] and was investigated to show the potential of dose-efficient reconstruction methods in comparison to FBP methods. Besides modeling photon statistics, our approach also models geometrical parameters like the volumetric extent of a voxel, the area of a detector element as well as the area of the focal spot. In addition, a regularization technique based on total variation (TV) minimization was applied during the iterations which accounts for unrealistic variations between neighboring voxels while preserving sharp edges. Thereby the model-based reconstruction aims at providing superior image quality, but at the cost of significantly increased computation time. The number of subsets and the strength of the regularization were chosen such that the results maintained at least at the spatial resolution of the analytical FBP reconstruction.

Both standard and iterative reconstructions were performed and evaluated separately for the soft-tissue lesion and microcalcification detection tasks. For μCa, a high-resolution reconstruction was performed with a voxel size of $(50\ \mu m)^3$ and a sharp kernel; for STL, a low resolution reconstruction was performed with 2×2 binned detector data and a voxel size of $(150\ mm)^3$ with a smooth filter kernel (Table 3). STL data were smoothed further with a 3D Gauss kernel of variable width. Additional reconstructions were performed with a voxel size of $(10\ \mu m)^3$ to determine the system modulation transfer function (MTF).

Table 3 Overview of different CT data acquisition and reconstruction modes

Mode	Focal spot size	Convolution kernel	Voxel size
STL	100 or 300 μm	Smooth	$(150\ \mu m)^3$
μCa	100 or 300 μm	Sharp	$(50\ \mu m)^3$

Phantoms

We employed a variety of phantoms mimicking the female breast with respect to shape, dimensions and tissue composition. A cylinder is reasonably well adapted to what we see in prone imaging by MRI and CT; the diameter was varied between 8 and 18 cm [22]. We used cylinders with a diameter of 14 cm and a length of 10 cm as a typical breast.

For the measurements of spatial resolution we used water cylinders with a 10 μm diameter tungsten (W) wire placed 2 mm off center (Fig. 2a). Profiles of the wire were acquired in an region of interest (ROI) of 1 mm in diameter and averaged over 180° to calculate the point spread function. From this the MTF was calculated and spatial resolution determined as the 10% value of the MTF.

To investigate the visibility of different lesions in the breast, a homogeneous phantom of 80% adipose and 20% glandular tissue [27], 14 cm in diameter and 10 cm in length representing an average breast [28], was modeled. A cylinder of adipose tissue, 30 mm in diameter, with glandular lesions with and without areas of microcalcification was placed inside (Fig. 2b,c). Soft-tissue lesions were chosen as spheres of 1, 2 and 5 mm in diameter with a contrast of glandular to adipose tissue around 120 HU. Areas of microcalcifications of 100, 150 and 200 μm in diameter were arranged in 2 mm diameter glandular tissue in clusters of three perpendicular rows of five spheres of the same size with a distance to each other equal to their diameter. The calcifications were assumed to be composed of calcium hydroxyapatite with a density of $3.16\ mg/cm^3$; their contrast in glandular tissue was around 5,000 HU at 60 kV.

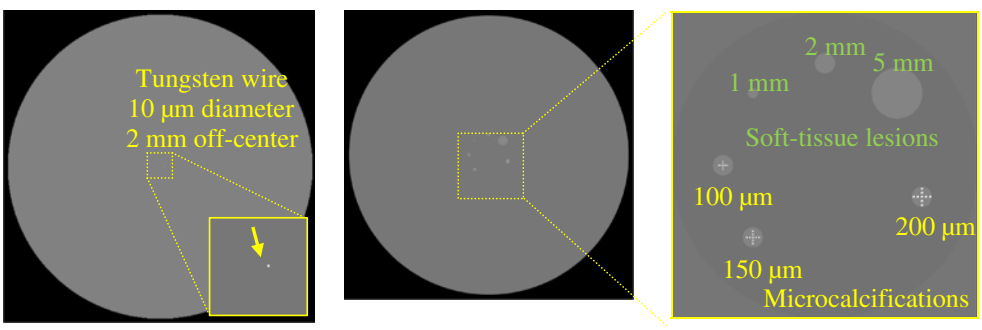

Fig. 2 Phantoms used to assess the performance of breast CT. (**a**) Water cylinder with a 10 μm tungsten wire placed 2 mm off center for MTF determination. (**b**) Homogeneous 14 cm diameter phantom with soft-tissue lesions and areas of microcalcification. (**c**) Magnified portion of (**b**) with the structures labeled

Simulations of CT images

Projections were simulated by ray-tracing using the software package ImpactSim (Artemis Imaging GmbH, Erlangen, Germany). Attenuation coefficients of the materials used for the simulations were calculated according to their elemental composition and the respective attenuation coefficients of the elements. To generate results as realistic as possible, we modeled the spatial extent of the focal spot and the area of the detector pixels as well as the motion of the gantry during the measurement of a projection. Scattered radiation was disregarded in view of the detector characteristics and the relatively small cone beam. Quantum noise reflecting the original intensity and the attenuation of the ray was added using Poisson-distributed noise to the projection data.

Simulations of 3D dose distributions

All dose calculations were carried out with the Monte Carlo tool ImpactMC (CT Imaging GmbH, Erlangen, Germany) validated previously [29]. For dose determination, coverage of the complete breast was assumed. For this, three circular scans with the distance equal to the collimation were modeled. The dose simulations traced 3.6×10^9 photon histories for each simulation resulting in a standard deviation of less than 2% for a voxel size of 1 mm^3.

For any specific parameter setting, i.e. for a specific mAs value and resulting air kerma value, the average dose absorbed in the whole breast results. This value is higher than the AGD, because the dose to the centrally located glandular tissue is lower than the dose in the periphery which is included in our estimate. We therefore remain on the safe side when estimating AGD by using the mean dose for the complete breast. Conversion factors of dose to air kerma for different breast diameters and, vice versa, the mAs values necessary for specific dose targets result and allow appropriate parameter selection. We selected an AGD of 3 mGy for the investigation presented below; i.e., we stayed below the typical values of 3.5 to 4 mGy for two-view mammography [21].

Results

Spatial resolution

The MTFs were determined in data sets reconstructed with a voxel size of $(150\ \mu m)^3$ and $(50\ mm)^3$, respectively, according to the definition of the STL and μCa protocols. Data were obtained for 100 and 300 μm focus size. Each scan was processed separately for STL and μCa analysis (Fig. 3). The desired resolution of 100 μm diameter details, corresponding to a resolution of 5 lp/mm, is demonstrated for both focus sizes. In STL reconstructions, resolution of about 300 μm is essentially the same for both focus sizes.

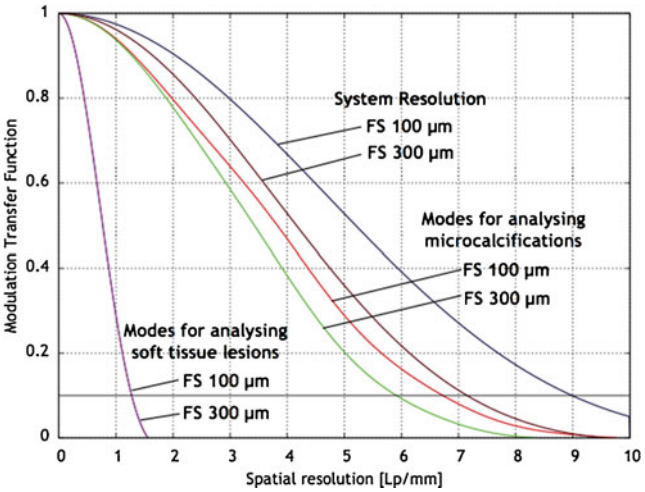

Fig. 3 Wire MTFs determined for STL and μCa reconstructions with both 100 and 300 μm focal spot sizes. In addition, system MTFs with both focal spot sizes are given

Noise

Noise results were determined for the same settings as in the MTF determination and in image quality assessments in the next section. Exemplary values of noise, determined in homogeneous regions in the center of the phantoms, are illustrated in Fig. 4. Noise levels were reduced significantly using MBIR reconstruction. As expected, noise reduction increased with resolution. E.g., in the STL case only about 20% noise reduction was achieved; with the μCa phantom a dose reduction of 80% was achievable.

Lesion detectability

According to the defined goals of investigating lesion detectability for STL and μCa, we simulated single CT data acquisitions with 100 and with 300 μm focal spot size at 3 mGy AGD and calculated the respective image volumes with $(150\ \mu m)^3$ and $(50\ \mu m)^3$ voxel size, respectively (Fig. 4a–d). In addition, MBIR reconstructions of the same data as in Fig. 4c,d were calculated (Fig. 4e,f). Glandular lesions in adipose tissue, marked by white arrows, were clearly visible in all cases for 2 and 5 mm diameter lesions (Fig. 4a,c,e). For all reconstructions, the 1 mm glandular lesion is not adequately visible. The glandular lesions containing areas of microcalcification, marked by yellow arrows, are well seen due to the high signal contributed by the μCa, although the calcified foci are not resolved as

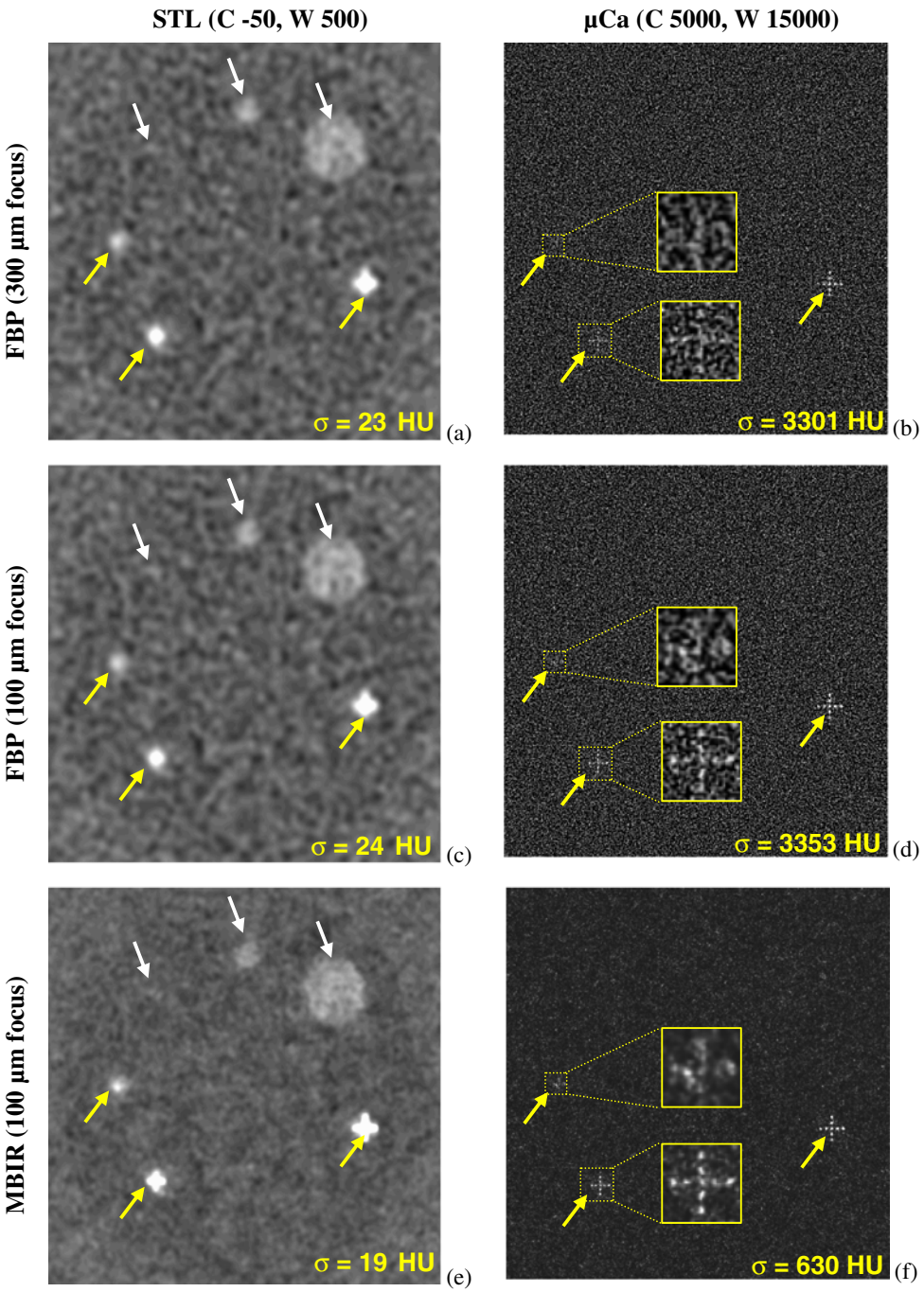

Fig. 4 Comparison of simulations with 300 and 100 µm focal spot size at 3 mGy AGD and FBP reconstruction (**a**–**d**). Significant differences are visible only for the µCa reconstruction with the large focal spot size (**b**) exhibiting decreased resolution compared to (**d**). The MBIR STL display (**e**) offers better resolution and the noise level reduced by about 20% (**c**). In the µCa mode, MBIR allows a noise reduction of about 80% and improvements in resolution for both 100 and 150 µm microcalcifications (**f**) as compared to (**d**)

single entities due to the low resolution in the STL mode. In the µCa reconstructions, the microcalcification patterns are well resolved down to 150 µm calcification diameter in all cases. The 100 µm calcifications are not shown with 300 µm focus size (Fig. 4b), but are recognizable for the 100 µm focus size with both analytic and iterative reconstruction (Fig. 4d,f). The constraint that MBIR provides resolution no worse than FBP, but often improved, can be verified by comparing Fig. 4d and f. Reconstruction times are short enough to be clinically realistic.

Discussion

The present study focused on the basic question whether comprehensive diagnosis of breast cancer matching the demands listed in Table 1 can be provided by CT. All results indicate that it should be possible. It had to be expected and was shown earlier that the first four demands can be met. From the start of the project, the big questions related to demands 5 and 6 on resolution and dose limits (Table 1).

For the selected geometry and detector concept with 100 μm pixel size, a detail resolution of 100 μm or better was demonstrated. Detectability of respective structures will depend on their contrast, however. For areas of microcalcification we have the favorable situation that contrasts of more than 5,000 HU can be expected and were verified at 60 kV [15]. Due to this high signal, the existence of microcalcification clusters is clearly recognizable even when they are not resolved as single entities (Fig. 4a,c,e). This finding can be used for a selective strategy: Start with a very low-dose overview CT data acquisition and follow up by high-resolution CT of a limited volume of interest. We have shown that this general approach can provide high resolution with reduced total dose [25]. Even the standard single-CT data acquisition approach appears to provide detectability of microcalcifications superior to mammography which may claim about 150 μm at best.

Regarding dose, taking AGD as a measure, our results indicate that CT will not need dose levels elevated over those of mammography screening. Earlier prototype studies in the USA, although operating at much lower resolution, recorded significantly higher dose [12]. Our favorable results have to be assigned to a strict optimization strategy with respect to dose efficiency: It relates to the choice and design of the components, primarily to the directly converting CdTe detector, to the spiral scan geometry, and to the versatile image reconstruction and data handling approach [23]. It should also be noted that, at equal AGD, CT will offer the advantage of a relatively homogeneous dose distribution, while mammography exhibits peak dose values at the entrance side which are typically several 100% higher than the AGD value [30]. With the rotation time of 2 s per 360°, total CT data acquisition time per breast will be below 10 s

Further work and confirmation is necessary regarding the assumptions on contrast. CT values of foci of microcalcification of about 5,000 HU in the simulations are realistic since we measured even higher values in micro-CT at the same voltage with lower filtration. With proper contrast medium injection an enhancement of about 120 HU can also be expected at 60 kV [14]. For soft-tissue contrast in general we still do not have sufficient data.

The influence of scattered radiation was disregarded in view of the detector characteristics and the limited cone beam. This assumption will have to be verified, but we can be certain that the scatter-to-primary ratios will be much lower than in flat-detector breast CT. We intend to design and use shaped filters from the start of operation, but did not include them in this study yet. They are expected to reduce both dose and scatter without an impact on image quality. Tube power requirements of 1 to 5 kW are to be expected depending on breast diameter and filtration. These demands can certainly be fulfilled for 300 μm focus size; work on novel x-ray tubes with smaller focal spots and increased power is underway. These would also be of interest if we have to offer even higher resolution. The possibility to do so without a dose penalty can make use of the VOI technique described above.

In conclusion, all performance features postulated in Table 1 appear to be realizable with the proposed design. Excellent spatial resolution of down to 100 μm was shown to be achievable. Resolution can be reduced in situations where high resolution is not required, in order to lower image noise for improved low-contrast imaging. Dose levels below the upper level of 5 mGy accepted for screening mammography are realistic. Soft-tissue lesion detection well below a diameter of 5 mm appears possible with and without the application of contrast media. Areas of microcalcification are easily detected as clusters even in the soft-tissue displays. Single microcalcified foci are quite visible down to a diameter of 150 μm. Experimental and clinical proof of device performance are planned late in 2011 and for 2012, respectively.

Acknowledgements The authors are grateful for the financial support of this work by the European Union [19], the Deutsche Forschungsgemeinschaft [20] and the Bundesministerium für Bildung und Forschung [31]. The results presented were produced in a cooperation of the Institute of Medical Physics and Artemis Imaging GmbH, a spinoff of the IMP and also located in Erlangen. Special thanks go to our colleagues Felix Althoff, Ronny Hendrych, Martin Hupfer, and Tristan Nowak for their tremendous support of this work.

W. Kalender is the founder, CEO and shareholder of Artemis Imaging GmbH, Erlangen, Germany.

M. Beister and D. Kolditz are part-time employees of Artemis Imaging, J. Boone is a consultant to Artemis Imaging.

References

1. Hall FM (2008) The rise and impending decline of screening mammography. Radiology 247:597–601
2. Smith JA, Andreopoulou E (2004) An overview of the status of imaging screening technology for breast cancer. Ann Oncol 15 (Suppl 1):18–26
3. Yaffe MJ (2004) What should the burden of proof be for acceptance of a new breast-cancer screening technique? Lancet 364(9440):1111–1112
4. Carney PA, Miglioretti DL, Yankaskas BC et al (2003) Individual and combined effects of age, breast density, and hormone replacement therapy use on the accuracy of screening mammography. Ann Intern Med 138:168–175
5. Kolb TM, Lichy J, Newhouse JH (2002) Comparison of the performance of screening mammography, physical examination, and breast US and evaluation of factors that influence them: an analysis of 27,825 patient evaluations. Radiology 225:165–175
6. Kuhl CK, Schrading S, Leutner CC et al (2005) Mammography, breast ultrasound, and magnetic resonance imaging for surveillance of women at high familial risk for breast cancer. J Clin Oncol 23:8469–8476
7. Gennaro G, Toledano A, di Maggio C et al (2010) Digital breast tomosynthesis versus digital mammography: a clinical performance study. Eur Radiol 20:1545–1553

8. Gur D, Abrams GS, Chough DM et al (2009) Digital breast tomosynthesis: observer performance study. American Journal of Roentgenology 193:586–591
9. Teertstra H, Loo C, van den Bosch M et al (2010) Breast tomosynthesis in clinical practice: initial results. Eur Radiol 20:16–24
10. Boone JM, Nelson TR, Lindfors KK, Seibert JA (2001) Dedicated breast CT: radiation dose and image quality evaluation. Radiology 221:657–667
11. Lindfors KK, Boone JM, Nelson TR, Yang K, Kwan ALC, Miller DF (2008) Dedicated breast CT: initial clinical experience. Radiology 246:725–733
12. O'Connell A, Conover DL, Zhang Y et al (2010) Cone-beam CT for breast imaging: radiation dose, breast coverage, and image quality. Am J Roentgenol 195:496–509
13. McCormack VA, dos Santos SI (2006) Breast density and parenchymal patterns as markers of breast cancer risk: a meta-analysis. Cancer Epidemiol Biomarkers Prev 15:1159–1169
14. Prionas ND, Lindfors KK, Ray S et al (2010) Contrast-enhanced dedicated breast CT: initial clinical experience. Radiology 256:714–723
15. Kalender WA (2009) High-resolution CT of the breast: a proposal! Eur Radiol 19(Suppl 4):849–852
16. European Reference Organisation for Quality Assured Breast Screening and Diagnostic Services (EUREF) (2008) European guidelines for quality assurance in breast cancer screening and diagnosis, Fourth Edition. http://www.euref.org/index.php?option=com_content\&view=article\&id=5\&Itemid=25. Accessed May 26, 2011
17. American College of Radiology (2008) ACR Practice guidline for performance of Screening and diagnostic mammography. http://www.acr.org/secondarymainmenucategories/quality_safety/guidelines/breast/screening_diagnostic.aspx. Accessed May 26, 2011
18. Yaffe MJ, Mainprize JG (2011) Risk of radiation-induced breast cancer from mammographic screening. Radiology 258:98–105
19. EC EURATOM 7th Framework Program "Dedicated CT of the female breast: Feasibility, optimization and comparison to competing imaging modalities", Contract No. FP/213153 (2008–2010) PI: W. A. Kalender. http://www.imp.uni-erlangen.de/BreastCT/index.html. Accessed May 26, 2011
20. Deutsche Forschungsgemeinschaft Research Unit FOR 661 "Multimodal Imaging for Preclinical Research", DFG Az. KA 1254/11-2 (2009–2012) PI: W. A. Kalender. http://www.imp.uni-erlangen.de/for661/index.htm. Accessed May 26, 2011
21. Hendrick RE, Pisano ED, Averbukh A et al (2010) Comparison of acquisition parameters and breast dose in digital mammogrphy and screen-film mammography in the American College of Radiology Imaging Network Digital Mammographic Imaging Screening Trial. Am J Radiology 194:362–369
22. Boone JM, Shah N, Nelson TR (2004) A comprehensive analysis of DgN[sub CT] coefficients for pendant-geometry cone-beam breast computed tomography. Med Phys 31:226–235
23. Kalender WA (2011) Computed tomography. Publicis Corporate Publishing, Erlangen
24. Weigel M, Vollmar SV, Kalender WA (2011) Spectral optimization for dedicated breast CT. Med Phys 38:114–124
25. Kolditz D, Kyriakou Y, Kalender WA (2010) Volume-of-interest (VOI) imaging in C-arm flat-detector CT for high image quality at reduced dose. Med Phys 37:2719–2730
26. Beekman FJ, Kamphuis C (2001) Ordered subset reconstruction for x-ray CT. Phys Med Biol 46:1835
27. International Commission on Radiation Units and Measurements (1989) ICRU report 44: tissue substitutes in radiation dosimetry and measurement
28. Yaffe MJ, Boone JM, Packard N et al (2009) The myth of the 50–50 breast. Med Phys 36:5437–5443
29. Deak PD, Langner O, Lell M, Kalender WA (2009) Effects of adaptive section collimation on patient radiation dose in multi-section spiral CT. Radiology 252:140–147
30. Sechopoulos I, Feng SSJ, D'Orsi CJ (2010) Dosimetric characterization of a dedicated breast computed tomography clinical prototype. Med Phys 37:4110–4120
31. Bundesministerium für Bildung und Forschung (BMBF) Spitzencluster Medical Valley, Verbund Bildgebende Diagnostik: Leitprojekt Brust CT, Az. 01EX1002 PI: W. A. Kalender